Degeneracy of the thermal properties of buried structures

A. Salazar,[a] F. Garrido, and A. Oleaga
Departamento de Física Aplicada I, Escuela Superior de Ingenieros, Universidad del Pais Vasco, Alameda Urquijo s/n, 48013 Bilbao, Spain

R. Celorrio
Departamento de Matemática Aplicada, Universidad de Zaragoza, Campus Río Ebro, Edificio Torres Quevedo, 50018 Zaragoza, Spain

(Received 7 April 2005; accepted 11 May 2005; published online 6 July 2005)

In thermal wave physics the surface temperature of a material depends on the thermal diffusivity and thermal effusivity of the components. Therefore these thermal properties of buried structures are expected to be retrieved from the measurement of the surface temperature using photothermal techniques. Then, from the constitutive equations, thermal conductivity and specific heat of the inclusions can be calculated. In this paper we demonstrate analytically that when the thermal properties of the inclusions are very different from those of the matrix they are degenerate. Three kinds of inclusions have been studied: layers, cylinders, and spheres. If the transport thermal properties of the inclusion are much higher (much lower) than those of the matrix; only its specific heat (thermal effusivity) can be retrieved. On the other hand, for a gas inclusion only its thermal conductivity can be determined. Photothermal measurements performed on three calibrated samples containing buried cylinders confirm the theoretical conclusions. © *2005 American Institute of Physics*. [DOI: 10.1063/1.1946914]

I. INTRODUCTION

Thermal wave physics is based on the generation and detection of thermal waves in the sample under study. Thermal waves are generated at the surface of an opaque material because of the absorption of an intensity-modulated light beam. As they propagate through the material they are scattered by the inclusions that are buried beneath the surface, in such a way that the surface temperature depends on their position, shape, and thermal properties. In order to reconstruct the geometry and thermal properties of the inclusions the first step is to solve the so-called forward problem, i.e., to calculate the surface temperature of the sample provided that the geometrical and thermal properties are known. This has been already performed for inclusions with simple shapes: planes, cylinders, and spheres.[1–3] The second step requires to develop an inverse procedure to retrieve the unknown properties of the inclusions from the knowledge of the surface temperature, which can be obtained by using some of the photothermal techniques: infrared radiometry, mirage effect, photothermal reflectance, etc.[4]

Two possibilities are found depending on the number of unknowns to be retrieved. For an infinite number of unknowns the inverse problem is ill posed. This means that the reconstructed properties are extremely sensitive to the starting experimental data. This is the case, for instance, of depth profiling in hardened steel, where the thermal properties vary as a function of depth.[5] On the contrary, for a finite number of unknowns the inverse problem is well posed and therefore the properties can be reconstructed properly. This is the case of layered structures, for which we are usually interested in determining the thermal properties of the layers, their depth and thickness, and the presence of thermal barriers between layers.[6] It is also the case of fiber-reinforced composites for which we are looking for the thermal properties of fibers and for the lack of adherence between fibers and matrix. The same is valid for particulate-reinforced composites. However, when the thermal properties of the inclusions (layers, cylinders, or spheres) are very different from those of the matrix the complete determination of the thermal properties of the inclusions cannot be performed.

In homogeneous and isotropic materials there are four thermal properties: specific heat (c), thermal conductivity (K), thermal diffusivity (D), and thermal effusivity (e). However, only two are linearly independent because of the constitutive equations $D=K/\rho c$ and $e=\sqrt{\rho c K}$. The specific heat is the only thermal property required in static experiments, i.e., when the temperature is independent of position and time. The thermal conductivity is the only thermal property required in steady problems, i.e., when the temperature does not vary with time. However, the temperature distribution in time-varying experiments depends on two thermal properties: D and e. This means that when using transient techniques (as is the case of the photothermal techniques) it is expected to retrieve both D and e, and from them to calculate ρc and K.

In this paper we demonstrate analytically, for three kinds of inclusions (layers, cylinders, and spheres), that a degeneracy of the thermal properties appears for three extreme cases: (1) If the transport thermal properties of the inclusions are much higher than those of the matrix the temperature distribution only depends on the specific heat of the inclusions, and therefore this is the only thermal property that can be retrieved; (2) if the transport thermal properties of the inclusions are much lower than those of the matrix the tem-

[a]Electronic mail: wupsahea@bi.ehu.es

perature distribution only depends on the thermal effusivity of the inclusions, therefore this is the only thermal property that can be retrieved; and (3) if the inclusions are gases (very low K, but high D) the temperature distribution only depends on the thermal conductivity of the gas, which is the only thermal property that can be retrieved. Photothermal measurements performed on three calibrated samples containing buried cylinders confirm the theoretical conclusions.

II. THEORY

A. Layered systems

Let us consider an opaque and stratified material made of n parallel layers ($i=1,n$) of thickness l_i, thermal diffusivity D_i, and thermal effusivity e_i that is illuminated by a light beam of intensity I_0 modulated at a frequency f ($\omega=2\pi f$). We assume that there is no thermal resistance between layers and that heat losses are negligible. The temperature at the illuminated surface can be written in an elegant way using the quadrupole method:[1]

$$T=\frac{I_0}{2}\frac{A}{C}, \tag{1}$$

where

$$\begin{pmatrix} A & B \\ C & E \end{pmatrix}=\prod_{j=1}^{n}\begin{pmatrix} A_j & B_j \\ C_j & E_j \end{pmatrix}, \tag{2}$$

with

$$A_j=E_j=\cosh(q_j l_j),\quad B_j=\frac{\sinh(q_j l_j)}{e_j\sqrt{i\omega}},$$
$$\text{and } C_j=e_j\sqrt{i\omega}\sinh(q_j l_j). \tag{3}$$

Here $q_j=\sqrt{i\omega/D_j}$ is the thermal wave vector.

The effect of a thermal resistance (R_{th}) between layers j and $j+1$ is accounted for by inserting in Eq. (2) the following matrix between the two adjacent matrices j and $j+1$:

$$\begin{pmatrix} 1 & R_{\text{th}} \\ 0 & 1 \end{pmatrix}. \tag{4}$$

As can be seen the surface temperature depends on the thermal diffusivity and effusivity of each layer. Therefore, it seems that these properties can be determined from the measurement of the surface temperature provided that an appropriate fitting procedure is used. However, this is not always possible.

Let us consider a simple three-layer system where layers 1 and 3 are made of the same matrix material and layer 2 is an inclusion whose thermal properties are to be determined. If the thermal properties of this layer are very different from those of the matrix, a degeneracy appears in such a way that the surface temperature only depends on one of the thermal properties. Three cases will be considered.

1. Buried layer of high thermal transport properties

In this case K_2, D_2, and e_2 are much higher than those of the matrix. Since D_2 is very high, $q_2 l_2 \to 0$ and therefore $\exp(\pm q_2 l_2)\approx 1\pm q_2 l_2$. This is valid for $|q_2 l_2|\leqslant 0.15$, with an error less than 1%. Taking into account that the effusivity can be rewritten as $e=\sqrt{\rho c K}=\rho c\sqrt{D}$, Eqs. (3) can be simplified as

$$A_2=E_2\approx 1,\quad B_2\approx\frac{l_2}{K_2}\approx 0,\quad \text{and } C_2\approx i\omega(\rho c l)_2, \tag{5}$$

which clearly indicates that the only thermal property of the inclusion layer that influences the surface temperature is the heat capacity through the factor $(\rho c l)_2$. Therefore neither K_2 nor D_2 can be determined from the measurement of T but its ratio.

2. Buried layer of low thermal transport properties

In this case K_2, D_2, and e_2 are much lower than those of the matrix. Since D_2 is very low, $q_2 l_2 \to \infty$ and therefore $\exp(-q_2 l_2)\approx 0$. This is valid for $|q_2 l_2|\geqslant 7$, with an error less than 1%. Accordingly, Eqs. (3) can be written as

$$A_2=E_2\approx\frac{1}{2}\exp(q_2 l_2),\quad B_2\approx\frac{1}{2}\frac{\exp(q_2 l_2)}{e_2\sqrt{i\omega}},$$
$$\text{and } C_2\approx\frac{1}{2}i\omega e_2\exp(q_2 l_2). \tag{6}$$

Substituting these values into Eq. (1) we have

$$T\approx\frac{I_0}{2}\frac{(A_1A_3+B_1C_3)e_2\sqrt{i\omega}+B_1A_3 i\omega e_2^2+A_1C_3}{(C_1A_3+E_1C_3)e_2\sqrt{i\omega}+E_1A_3 i\omega e_2^2+C_1C_3}, \tag{7}$$

showing that the only thermal property of the buried layer that influences the surface temperature is the thermal effusivity e_2.

3. Buried layer of gas

Now K_2, e_2, and $(\rho c)_2$ are very low, but the thermal diffusivity D_2 is high, actually similar to that of metals. Consequently, $\exp(\pm q_2 l_2)\approx 1\pm q_2 l_2$, and substituting in Eqs. (3) we obtain

$$A_2=E_2\approx 1,\quad B_2\approx\frac{l_2}{K_2},\quad \text{and } C_2\approx i\omega(\rho c l)_2\approx 0, \tag{8}$$

indicating that the only thermal property of the inclusion layer that influences the surface temperature is the thermal conductivity through the factor $(l/K)_2$.

B. Buried cylinders

Let us now consider an infinite cylinder of radius a buried at a depth d beneath the surface of an opaque and semiinfinite material that is illuminated by a light beam of intensity I_0 modulated at a frequency f ($\omega=2\pi f$). The geometry of the problem is shown in Fig. 1. We take into consideration that there could be a lack of adherence between the cylinder and matrix by introducing a thermal contact resistance R_{th} between them. On the other hand, we assume that heat losses are negligible. In the following, indices M and C stand for matrix and cylinder, respectively. The surface temperature can be written as[2]

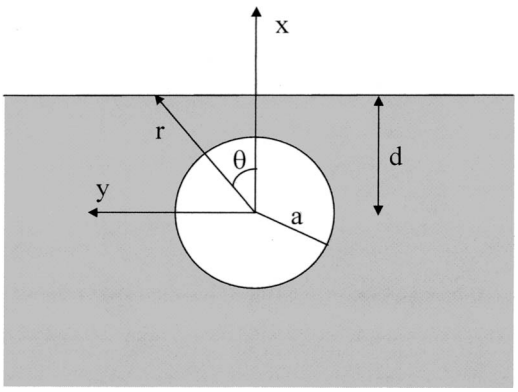

FIG. 1. Geometry of a semi-infinite material containing a buried cylinder.

$$T(r,\theta) = \frac{I_0 i}{2K_M q_M} e^{iq_M(d-r\cos\theta)} + 2\sum_{m=-\infty}^{\infty} A_m H_m(q_M r) e^{im\theta}, \tag{9}$$

where H_m are the mth order of the Hankel functions of the first kind. The first term in Eq. (9) represents the incident plane thermal wave starting at the sample surface, while the second one accounts for the scattered waves coming out from the cylinder. Equation (9) requires the knowledge of the $2m+1$ constants A_m $(m=-\infty,\infty)$ that can be obtained from the $2m+1$ equations given by the boundary conditions at the cylinder surface (existence of a thermal resistance and heat flux continuity):[2]

$$A_m \frac{1 - Y_m^C/Z_m^C}{S_m^M - Z_m^M Y_m^C/Z_m^C} + \sum_{n=-\infty}^{\infty} A_n H_{m+n}(2q_M d) = -\frac{I_0 i}{2K_M q_M} e^{iq_M d} i^{-m}, \tag{10}$$

where

$$S_m^M = \frac{J_m(q_M a)}{H_m(q_M a)}, \quad Z_m^M = \frac{J'_m(q_M a)}{H'_m(q_M a)},$$

$$Y_m^C = \frac{J_m(q_C a) + K_C R_{\text{th}} J'_m(q_C a)}{H_m(q_M a)}, \tag{11}$$

$$\text{and } Z_m^C = \frac{K_C}{K_M}\frac{J'_m(q_C a)}{H'_m(q_M a)},$$

J'_m and H'_m being the derivatives of the Bessel and Hankel functions, respectively.

It is worth noting that the contribution of the cylinder to the surface temperature only appears in the ratio Y_m^C/Z_m^C that according to Eqs. (11) can be written as

$$\frac{Y_m^C}{Z_m^C} = \frac{K_M H'_m(q_M a)}{H_m(q_M a)}\left[\frac{J_m(q_C a)}{K_C J'_m(q_C a)} + R_{\text{th}}\right], \tag{12}$$

where the factor inside the parentheses incorporates the influence of the geometrical and thermal properties of the buried cylinder. Now we analyze the value of this factor for the same three extreme cases studies for layered systems.

1. Buried cylinder of high thermal transport properties

In this case $q_C a \to 0$ and $K_C \to \infty$. Using the asymptotic behavior of the Bessel functions and its derivatives[7] we obtain

$$\frac{J_0(q_C a)}{K_C J'_0(q_C a)} \approx -\frac{2}{i\omega(\rho c a)_C}$$

and

$$\frac{J_m(q_C a)}{K_C J'_m(q_C a)} \approx \frac{a}{K_C |m|} \to 0, \quad \text{if } m \neq 0. \tag{13}$$

This approach is valid, within an error less than 1%, provided $|q_C a| \leqslant 0.28$. Equation (13) indicates that only the factor $(\rho c a)_C$ influences the surface temperature. This means that neither K_C nor D_C can be determined.

2. Buried cylinder of low thermal transport properties

In this case $q_C a \to \infty$. Using the asymptotic behavior of the Bessel functions and its derivatives[7] we obtain

$$\frac{J_m(q_C a)}{K_C J'_m(q_C a)} \approx \frac{1}{(1-i)\sqrt{\pi f} e_C}, \quad \forall\, m, \tag{14}$$

that is valid, within an error less than 1%, provided $|q_C a| \geqslant 35$. Therefore the only thermal property of the cylinder that influences the surface temperature is the effusivity e_C.

3. Buried cylinder of gas

In this case $q_C a \to 0$ and $K_C \to 0$. Therefore

$$\frac{J_0(q_C a)}{K_C J'_0(q_C a)} \approx -\frac{2}{i\omega(\rho c a)_C} \to -\infty$$

and

$$\frac{J_m(q_C a)}{K_C J'_m(q_C a)} \approx \frac{a}{K_C |m|}, \quad \text{if } m \neq 0, \tag{15}$$

indicating that only the factor $(a/\dot{K}_C)$ could be calculated.

C. Buried spheres

Finally, we consider a sphere of radius a buried at a depth d beneath the surface of an opaque and semi-infinite material that is illuminated by a light beam of intensity I_0 modulated at a frequency f $(\omega = 2\pi f)$. The geometry of the problem is shown in Fig. 2. We take into consideration that there could be a lack of adherence between sphere and matrix by introducing a thermal contact resistance R_{th} between them. On the other hand, we assume that heat losses are negligible. In the following, indices M and S stand for matrix and sphere, respectively. The surface temperature can be written as[3]

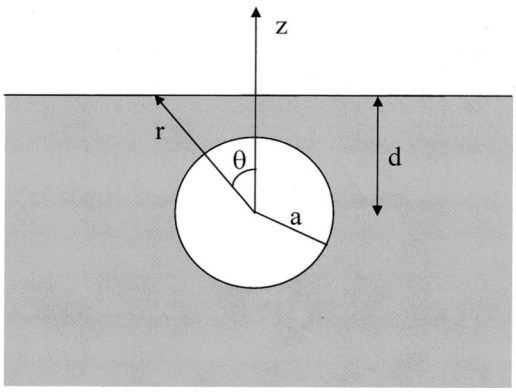

FIG. 2. Geometry of a semi-infinite material containing a buried sphere.

$$T(r,\theta) = \frac{I_0 i}{2K_M q_M} e^{iq_M(d-r\cos\theta)} + 2\sum_{m=0}^{\infty} B_m h_m(q_M r) P_m(\cos\theta), \tag{16}$$

where h_m are the mth order of the spherical Hankel functions of the first kind and P_m the Legendre functions. The first term in Eq. (16) represents the incident plane thermal wave starting at the sample surface, while the second one accounts for the scattered waves coming out from the sphere. Equation (16) requires the knowledge of the $m+1$ constants B_m $(m=0,\infty)$ that can be obtained from the $m+1$ equations given by the boundary conditions at the sphere surface (existence of a thermal resistance and heat flux continuity):[3]

$$B_m \frac{1 - Y_m^S/Z_m^S}{S_m^M - Z_m^M Y_m^S/Z_m^S} + \sum_{n=0}^{\infty} (-1)^n B_n Q_{0,m,0n}(2d) = -\frac{I_0 i}{2K_M q_M} e^{iq_M d}(1+2m) i^{-m}, \tag{17}$$

where

$$S_m^M = \frac{j_m(q_M a)}{h_m(q_M a)}, \quad Z_m^M = \frac{j'_m(q_M a)}{h'_m(q_M a)}, \qquad Y_m^S = \frac{j_m(q_S a) + K_S R_{\text{th}} j'_m(q_S a)}{h_m(q_M a)}, \quad Z_m^S = \frac{K_S}{K_M}\frac{j'_m(q_S a)}{h'_m(q_M a)}, \tag{18}$$

j'_m and h'_m being the derivatives of the spherical Bessel and Hankel functions, respectively.

As in the case of cylinders, the contribution of the sphere to the surface temperature only appears in the ratio Y_m^S/Z_m^S, that according to Eqs. (18) can be written as

$$\frac{Y_m^S}{Z_m^S} = \frac{K_M h'_m(q_M a)}{h_m(q_M a)}\left[\frac{j_m(q_S a)}{K_S J'_m(q_S a)} + R_{\text{th}}\right], \tag{19}$$

where the factor inside the parentheses incorporates the influence of the geometrical and thermal properties of the buried sphere. Now we analyze the value of this factor for the same three extreme cases we are dealing with.

1. Buried sphere of high thermal transport properties

In this case $q_S a \to 0$ and $K_S \to \infty$. Using the asymptotic behavior of the spherical Bessel functions and its derivatives[7] we obtain

$$\frac{j_0(q_S a)}{K_S j'_0(q_S a)} \approx -\frac{3}{i\omega(\rho c a)_S}$$

and

$$\frac{j_m(q_S a)}{K_S j'_m(q_S a)} \approx \frac{a}{K_S m} \to 0, \quad \text{if } m \neq 0. \tag{20}$$

This approach is valid, within an error less than 1%, provided $|q_S a| \leqslant 0.28$. Equation (20) indicates that only the factor $(\rho c a)_S$ influences the surface temperature. This means that neither K_S nor D_S can be determined.

2. Buried sphere of low thermal transport properties

In this case $q_S a \to \infty$ except for very small sphere. Using the asymptotic behavior of the spherical Bessel functions and its derivatives[7] we obtain

$$\frac{j_m(q_S a)}{K_S j'_m(q_S a)} \approx \frac{1}{(1+i)\sqrt{\pi f} e_S}, \tag{21}$$

which is valid within an error less than 1%, provided $|q_S a| \geqslant 35$. Therefore the only thermal property of the cylinder that influences the surface temperature is the effusivity e_S.

3. Buried sphere of gas

In this case $q_S a \to 0$ except for very big sphere. Therefore

$$\frac{j_0(q_S a)}{K_S j'_0(q_S a)} \approx -\frac{3}{i\omega(\rho c a)_S} \to -\infty$$

and

$$\frac{j_m(q_S a)}{K_S j'_m(q_S a)} \approx \frac{a}{K_S m}, \quad \text{if } m \neq 0, \tag{22}$$

indicating that the only the factor (a/K_C) could be calculated.

Before finishing this section let us remark that the same conclusions are valid for an unlimited number of cylinders or spheres embedded in a matrix slab. Moreover, these conclusions are also valid in flash thermography, where the sample surface is heated by a short duration laser pulse and the surface temperature is recorded as a function of time. Actually, to convert Eqs. (1), (9), and (16) to be used under pulsed conditions we proceed as follows.[8] As a first step $i\omega$ is replaced by $-s$, the Laplace variable, and $I_0/2$ by Q, the energy density of the light pulse, in the expression of the modulated temperature $T(\omega)$ to obtain the Laplace transform of the solution $T(s)$. Then, $T(t)$ can be obtained by the inversion of the Laplace transform, for instance, using the Stehfest algorithm.[9] During this process the approaches for the three extreme cases we are dealing with remain unchanged, and therefore the conclusions, too.

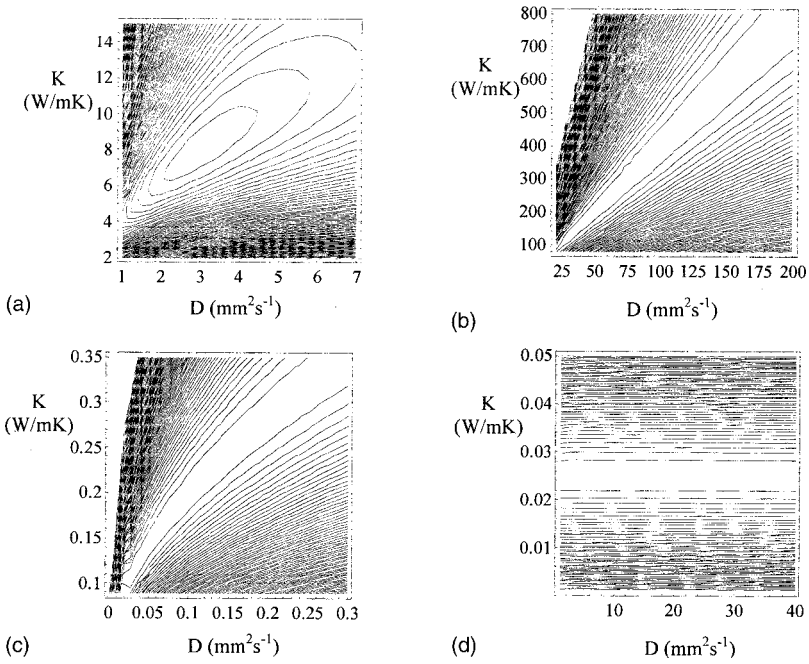

FIG. 3. Theoretical contour plots of the residual function g for a for a matrix material ($l=2$ mm, $K=3$ W m^{-1} K^{-1}, and $D=1$ mm^2 s^{-1}) that contains a 0.5-mm-thick layer, buried at a depth of 0.2 mm beneath the surface, with various thermal properties: (a) $K=8$ W m^{-1} K^{-1} and $D=3$ mm^2 s^{-1}, (b) $K=400$ W m^{-1} K^{-1} and $D=100$ mm^2 s^{-1}, (c) $K=0.2$ W m^{-1} K^{-1} and $D=0.1$ mm^2 s^{-1}, and (d) $K=0.025$ W m^{-1} K^{-1} and $D=22$ mm^2 s^{-1}.

III. INVERSE PROBLEM

In Sec. II we have obtained expressions for the surface temperature of a material with buried layers, cylinders, or spheres, provided the geometrical and thermal properties are known. However, from a practical point of view, it is more interesting to solve the inverse problem to extract information about the geometrical and thermal properties of both matrix and inclusions from the measurement of the surface temperature. To do this we use a nonlinear least-squares fitting procedure. Since in this work we are interested in the restrictions of the photothermal techniques to retrieve the thermal properties of the inclusions, we define a residual function of the thermal properties of the buried object as follows:

$$g(K,D)=\frac{1}{2}\sum_{j=1}^{N}|T_{\text{theory}}(K,D,f_j)-T_{\text{measured}}(f_j)|^2, \tag{23}$$

where T_{measured} is the experimental value of the surface temperature (amplitude or phase) at a frequency f_i and T_{theory} is the theoretical value at that frequency, calculated by means of the Eqs. (1), (9), and (16). The sum runs over all N modulation frequencies of the experiment.

Now, the determination of the thermal properties of the inclusion (K,D) is reduced to finding the set of parameters that minimizes g. To visualize this function we show in Fig. 3 its contour plot for a matrix material ($l=2$ mm, $K=3$ W m^{-1} K^{-1}, and $D=1$ mm^2 s^{-1}) that contains a 0.5-mm-thick layer, buried at a depth of 0.2 mm beneath the surface, with various thermal properties. T_{measured} has been simulated by adding a 2% random error to the calculated value of Eq. (1). In Fig. 3(a) we show the case of a buried layer whose thermal properties are close to those of the matrix: $K=8$ W m^{-1} K^{-1} and $D=3$ mm^2 s^{-1}. As can be seen a clear minimum appears, indicating that both K and D could be retrieved using an appropriate inversion algorithm. In Fig. 3(b) we show the case of a buried layer whose thermal properties are much higher than those of the matrix: $K=400$ W m^{-1} K^{-1} and $D=100$ mm^2 s^{-1}. Now there is not a minimum but a straight line that minimizes the residual function g. This means that, as predicted in Sec. II A 1, K and D are degenerate and only the ratio between them $\rho c=K/D=4\times10^6$ J m^{-3} K^{-1} could be retrieved. Figure 3(c) shows the case of a buried layer whose thermal properties are much lower than those of the matrix: $K=0.2$ W m^{-1} K^{-1} and $D=0.1$ mm^2 s^{-1}. Now there is not a minimum either, but a curve ($K=632\sqrt{D}$) that minimizes the residual function g. As before, K and D are degenerate and only the ratio $e=K/\sqrt{D}=632$ W s$^{-1/2}$ m^{-2} K^{-1} could be retrieved. Finally, Fig. 3(d) shows the case of a gas layer: $K=0.025$ W m^{-1} K^{-1} and $D=22$ mm^2 s^{-1}. As can be seen, there is not a minimum but a horizontal straight line ($K=0.025$) that minimizes g. This means that K could be retrieved while D remains completely unknown.

To find the minimum of the residual function we have used the Levenberg–Marquardt method that is a trust-region modification of the Gauss–Newton algorithm.[10,11] This method combines the advantages of the Gauss–Newton method (high order of convergence) and the steepest descent method (large region of convergence).

IV. EXPERIMENTAL RESULTS AND DISCUSSION

The validity of the model developed in previous sections has been tested experimentally by measuring the surface temperature of three calibrated samples containing a buried cylinder. Sample A has been prepared by embedding a stainless-steel fiber ($K_M=60$ W m^{-1} K^{-1}, $D_M=18$ mm^2 s^{-1}, and $a=250$ μm) inside a black epoxy ($K_M=0.10$ W m^{-1} K^{-1}, $D_M=0.12$ mm^2 s^{-1}, and d-$a=110$ μm). Sample B has been made by drilling a cylindrical air hole in the same black epoxy ($a=250$ μm and d-$a=110$ μm) and filling this hole with a slight smaller stainless-steel rod. Finally, sample C has been prepared by drilling an air cylindri-

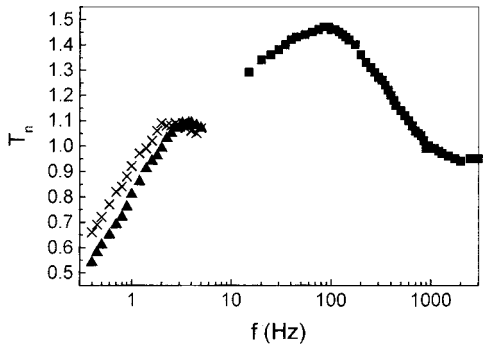

FIG. 4. Frequency dependence of the normalized temperature amplitude T_n just above the center of the cylinder for three calibrated samples: sample A (triangles), sample B (crosses), and sample C (squares).

cal hole in a carbon matrix (rigid graphite with purity of 99.95%, $K_M=150$ W m^{-1} K^{-1}, $D_M=95$ mm^2 s^{-1}, $a=250$ μm, and d-$a=160$ μm).

The surface temperature of these three samples has been measured using an infrared radiometry microscope whose scheme and performance have been described in detail elsewhere.[12] A multimode Nd:yttrium aluminum garnet (YAG) laser (1.06 μm) modulated by a mechanical chopper has been used to heat the sample surface. Its beam has been defocused to a diameter of 2 cm to guarantee that plane thermal waves are generated at the sample surface. The emitted infrared radiation from the sample surface has been collected by a gold-mirrored catadioptric microscope objective and focused with a ZnSe lens onto a liquid-nitrogen-cooled HgCdTe detector. The detector signal is preamplified before being sent to a lock-in amplifier, whose amplitude and phase are recorded. Modulation frequencies have been selected according to the thermal properties of the samples: low frequencies for black epoxy ($f=0.4-10$ Hz) and medium frequencies for graphite ($f=20-3000$ Hz). According to the size of the infrared detector and the optical magnification of the system, the surface temperature is collected from a square spot of 25 μm/side. Spatial scans have been performed by keeping fixed the heating beam while moving the sample with a micrometer translator. Frequency scans have been performed at two positions: just above the center of the cylinder (that corresponds to the highest or lowest temperature of the spatial scans) and far away from the cylinder (in the region where the surface temperature is not affected by the subsurface cylinder).

The surface temperature is normalized with respect to the temperature at a point far away from the cylinder. In Fig. 4 we show the frequency dependence of the normalized temperature amplitude T_n just over the center of the cylinder for the three calibrated samples. As expected the temperature in the graphite sample is higher than 1.0 (the matrix is a better conductor than the cylinder) while the temperature is less than 1.0 in the epoxy samples (the matrix is a worse conductor than the cylinder).[2] In Fig. 5 the experimental contour plots of the residual function g [Eq. (23)] of the surface temperature for the three calibrated samples are shown. Figure 5(a) corresponds to sample A, where no closed contours are found, but a long valley that minimizes g. Therefore, as predicted in Sec. II B 1, K and D of the steel fibers are degenerate and only their ratio, the heat capacity, $\rho c=K/D=3.3\times10^6$ J m^{-3} K^{-1}, can be measured.

Sample B is similar to sample A but between the steel rod and the epoxy matrix there is not a perfect thermal contact. We test the ability of the photothermal radiometry to retrieve the heat capacity and the thermal contact resistance. Figure 5(c) shows the contour plots of the residual function g of the temperature amplitude, where a minimum can be seen. However, the needlelike shape of the closed contours indicates a certain degree of degeneracy in the retrieval of the ρc, but a better resolution of R_{th}. Using the Levenberg–Marquardt method and starting from three different points (dots, squares, and crosses) we obtain $R_{\text{th}}=2.6\times10^{-4}$ m^2 K W^{-1} and $\rho c=2.3\times10^6$ J m^{-3} K^{-1}. Note that this last value is far from the real one $\rho c=3.3$

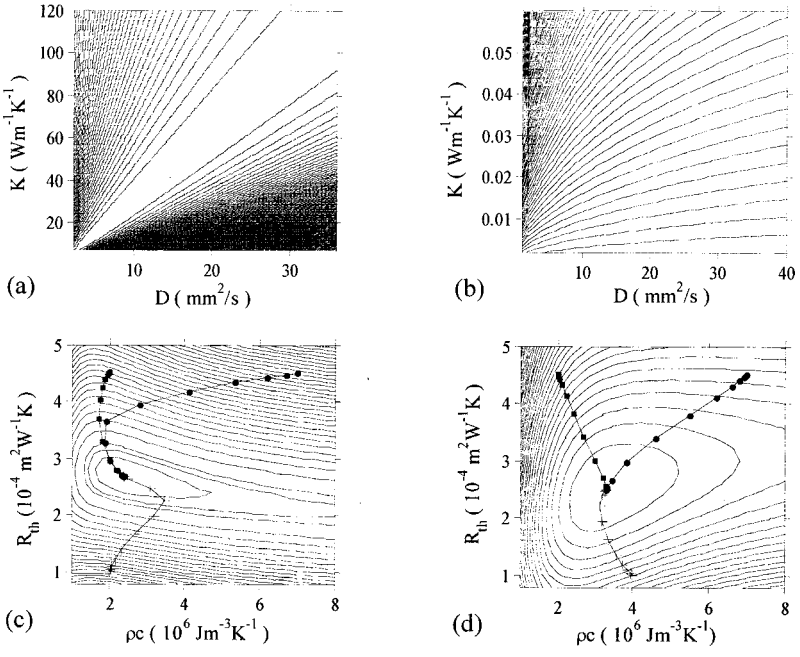

FIG. 5. Experimental contour plots of the residual function g for the three calibrated samples. (a) sample A, (b) sample C, (c) sample B for the amplitude, and (d) sample B for the phase.

$\times 10^6$ J m^{-3} K^{-1}. This uncertainty is related to sensibility of Eq. (23) to the noise level of the experimental data. Figure 5(d) is the same as Fig. 5(c) but for the temperature phase. Now a clearer minimum than in the case of the amplitude appears. Using the Levenberg–Marquardt method and starting from three different points we obtain $R_{th}=2.5 \times 10^{-4}$ m^2 K W^{-1} and $\rho c=3.4\times 10^6$ J m^{-3} K^{-1}. Note that using phase data we retrieve a similar R_{th} value, but we obtain the actual value of ρc. This means that phase data are less affected by degeneracy than amplitude data and therefore they will be preferred for inversion procedure.

The contour plots of the residual function of the temperature amplitude for sample C are shown in Fig. 5(b). There is neither closed contours nor a minimum of the residual function along a horizontal straight line as it was predicted in Sec. II B 3 [see Fig. 3(d)]. This is due to the fact that the surface temperature is almost insensitive to changes in the thermal conductivity of the gas cylinder (that is much lower than the thermal conductivity of the matrix) and therefore even small experimental noise destroys the convergence of the residual function. Accordingly, neither K nor D can be determined.

Photothermal techniques are used to measure the thermal properties of a wide variety of materials. Moreover, they can also be used to retrieve the thermal properties of subsurface structures, as is the case of delaminations, inclusions, voids, fibers, hardened steel, etc. When an infinite number of unknowns are to be obtained (ill-posed problem) inversion procedures are highly sensitive to the experimental noise, and unknowns are retrieved with poor accuracy. In this work we have demonstrated that even in well-posed problems, in which the number of unknowns is finite and therefore one expects to calculate them with high accuracy, there are some limitations imposed by the degeneracy of the thermal parameters. This degeneracy appears when the difference in thermal properties between matrix and inclusions is very high. Although they could be expected to be of minor practical interest, these extreme configurations are usually found both in nature (delaminations, voids, porosity, etc.) and in new composite materials (carbon fiber reinforced polymers, particulate reinforced composites, etc.) that are designed to improve mechanical and thermal properties.

ACKNOWLEDGMENTS

This work has been supported by the Ministerio de Ciencia y Tecnología through Research Grant No. MAT2002-04153-C02-01 (50% FEDER funds). One of the authors (F.G.) acknowledges a predoctoral fellowship from Universidad del País Vasco.

[1] D. Maillet, S. André, J. C. Batsale, A. Degiovanni, and C. Moyne, *Thermal Quadrupoles* (Wiley, New York, 2000).
[2] J. M. Terrón, A. Salazar, and A. Sánchez-Lavega, J. Appl. Phys. **91**, 1087 (2002).
[3] F. Garrido and A. Salazar, J. Appl. Phys. **95**, 140 (2004).
[4] D. P. Almond and P. M. Patel, *Photothermal Science and Technology* (Chapman and Hall, London, 1996).
[5] C. Glorieux, R. Li Voti, J. Thoen, M. Bertolloti, and C. Sibilia, Inverse Probl. **15**, 1149 (1999).
[6] C. Glorieux, J. Fivez, and J. Thoen, J. Appl. Phys. **73**, 684 (1993).
[7] *Handbook of Mathematical Functions*, edited by M. A. Abramowitz and I. A. Stegun (National Bureau of Standards, Washington DC, 1964).
[8] J.-C. Krapez, J. Appl. Phys. **87**, 4514 (2000).
[9] B. Davies, *Integral Transforms and Their Applications*, Texts in Applied Mathematics Vol. 41, 3rd ed. (Springer, Berlin, 2002).
[10] D. W. Marquardt, SIAM J. Appl. Math. 11, 431 (1963).
[11] Å. Björck, *Numerical Methods for Least Squares Problems* (SIAM, Philadelphia, PA, 1996).
[12] A. Ocáriz, A. Sánchez-Lavega, and A. Salazar, J. Appl. Phys. **81**, 7561 (1997).